

Self-sensing of flexural strain and damage in carbon fiber polymer-matrix composite by electrical resistance measurement

Shoukai Wang, D.D.L. Chung *

Composite Materials Research Laboratory, University at Buffalo, State University of New York, Buffalo, NY 14260-4400, USA

Received 28 January 2006; accepted 31 March 2006

Available online 19 May 2006

Abstract

The self-sensing of flexural strain and damage has been demonstrated in carbon fiber polymer-matrix composite by measuring the DC electrical resistance. Upon strain in the elastic regime, the compression surface resistance decreases reversibly (due to increase in the current penetration), while the tension surface resistance increases reversibly (due to decrease in the current penetration), and the oblique resistance increases reversibly. Upon minor damage, (i) the oblique resistance after unloading decreases, (ii) the oblique resistance decreases during load increase near the start of loading, and (iii) the curve of the oblique resistance or the resistance of the tension or compression surface vs. deflection becomes nonlinear. Upon major damage, all resistances abruptly and irreversibly increase, such that the onset occurs earlier for the compression surface resistance and the oblique resistance than the tension surface resistance. The surface resistances are superior indicators of strain, whereas the oblique resistance is a superior indicator of damage.
© 2006 Elsevier Ltd. All rights reserved.

Keywords: Carbon composites; Carbon fibers; Electrical (electronic) properties; Mechanical properties; Fracture

1. Introduction

The sensing of strain or stress in a structure is valuable for structural vibration control, load monitoring and load history recording. The sensing of damage is valuable for structural health monitoring, timely repair and safety enhancement.

Strain and stress are proportional to one another in the elastic regime. In the inelastic regime, the strain is not totally reversible, so that a portion of the strain is reversible and a portion is irreversible. At a sufficiently high stress in the inelastic regime, damage occurs. However, damage due to fatigue may occur at a low stress amplitude. In order to understand the cause of damage, knowledge of the stress/strain condition during damage infliction and record of the stress/strain history prior to damage infliction are useful.

The ability to sense both damage and stress/strain is necessary for correlating damage and stress/strain information. This ability is superior to that of sensing either damage alone or stress/strain alone. For example, acoustic emission allows damage infliction sensing, but it does not allow stress/strain sensing in the absence of damage [1–3]; ultrasonic inspection allows damage (crack) sensing, but it does not allow stress/strain sensing [4–6]. In contrast, electrical resistance measurement can provide simultaneous sensing of both damage and stress/strain, because damage and stress/strain have different effects on the resistance, as shown in composite materials that are not electrically insulating, such as continuous carbon fiber (aligned) polymer-matrix composites [7–29] and short carbon fiber (not aligned) cement-matrix composites [30–34].

This work is focused on continuous carbon fiber polymer-matrix composites, due to their importance for lightweight structures such as aircraft, missiles, satellites and sporting goods. By using electrical resistance measurement, the ability of these composites to sense their own strain and damage (i.e., self-sensing) under uniaxial tension has been

* Corresponding author. Tel.: +1 716 645 2593x2243; fax: +1 716 645 3875.

E-mail address: ddlchung@buffalo.edu (D.D.L. Chung).

demonstrated [11]. Their ability to sense their impact (drop impact) damage has also been demonstrated [35]. However, flexural strain and damage have not been addressed, in spite of the fact that flexure is one of the most common types of loading for structures. In particular, flexural loading is more commonly encountered than uniaxial tensile loading.

Flexure is more complicated than uniaxial tension in that the strain/stress is non-uniform. Under flexure, one surface is under compression while the opposite surface is under tension. As a result, the surface resistance should be measured under flexure, whereas either the volume resistance or the surface resistance can be measured under uniaxial tension. In the case of flexure, by separately measuring the surface resistance of the tension and compression surfaces, the strain and damage of each of these two surfaces can be determined.

Impact by dropping a weight on the top surface of a specimen inflicts damage, provided that the impact energy is sufficiently high. The damage is accompanied by indentation, which is an irreversible strain effect. Both damage and strain due to impact are localized. In contrast, the strain is spread out, though non-uniform, in flexure, and the strain is spread out and uniform in uniaxial tension. Due to the high speed associated with impact, strain effect in the elastic regime cannot be conveniently measured by the electrical resistance method. Therefore, damage sensing without strain sensing has been attained by resistance measurement for the case of impact [35]. Because of the difference in damage condition between the top surface (surface receiving the impact) and the bottom surface, surface resistance measurement is relevant.

This paper is aimed at demonstrating strain and damage self-sensing in a continuous carbon fiber polymer-matrix composite under flexure. A secondary objective relates to investigation of the damage and its evolution under flexure at various stress amplitudes for the purpose of understanding the mechanism and process of damage.

Due to its non-destructive nature and fast response, electrical resistance measurement is attractive for damage evolution study, as previously shown under tension–tension fatigue [28]. Tension–tension fatigue damage that is associated with a decrease in the tensile modulus is indicated by an irreversible increase in the volume electrical resistivity [28]. In the case of flexure, the ability of the electrical resistance method to probe the compression surface, the tension surface and the interior simultaneously during loading is particularly attractive for damage evolution investigation.

In this work, the conditions of the compression surface, tension surface and interior are indicated by the compression surface resistance, the tension surface resistance and the oblique resistance, respectively. The oblique resistance is the volume resistance in a direction at an angle ($<90^\circ$) to the surface, as measured by using two electrical contacts on each of the compression and tension surfaces, such that the contacts on the two surfaces are not directly opposite



Fig. 1. Schematic of the edge of a composite to illustrate the concept behind the placement of electrical contacts. A_1 , A_2 , A_3 , A_4 are contacts on one surface; B_1 , B_2 , B_3 and B_4 are contacts on the opposite surface. All the contacts are strips of about 2 mm wide in the direction perpendicular to the length of the composite.

one another. As illustrated in Fig. 1, contacts A_1 , A_2 , A_3 and A_4 allow measurement of the top surface resistance using the four-probe method; contacts B_1 , B_2 , B_3 and B_4 allow measurement of the bottom surface resistance; contacts A_1 and B_4 (as current contacts) and A_2 and B_3 (as voltage contacts) allow measurement of the oblique resistance. Because the line connecting A_1 and B_4 does not overlap exactly the line connecting A_2 and B_3 , the oblique resistance thus measured is not exact. Nevertheless, it gives valuable information about the interior condition of the specimen.

2. Experimental methods

The composite was a commercially manufactured 24-lamina quasi-isotropic $[0/45/90/-45]_{3s}$ laminate with IM7 carbon fiber (Hexcel Corp., PAN-based, intermediate modulus of 290 GPa, diameter 5 μm , 12,000 fibers per tow) and 977-3 epoxy (CYCOM, toughened epoxy resin with a curing temperature of 177 $^\circ\text{C}$). The self-sensing demonstration involved subjecting a composite laminate specimen of size $100 \times 10 \times 3.2$ mm to repeated three-point bending at progressively increasing flexural stress amplitudes (i.e., progressively increasing maximum deflection). Three loading cycles were carried out at each stress amplitude, which was progressively increased, with about 20 successive values that ranged from 22 MPa to the failure stress amplitude. At the highest stress amplitude, failure occurred during stress cycling. The span in the three-point bending was 80 mm, as shown in Fig. 2(a). The surface electrical resistances at both tension and compression sides of the specimen (as obtained by using all four contacts on the same surface of the specimen) and the oblique resistance (as explained in the Introduction and obtained by using two contacts on each of the two opposite surfaces, i.e., A and B on one surface and C and D on the opposite surface) were separately and continuously measured during loading and unloading by using silver paint in conjunction with copper wire as electrical contacts. The parts of the specimen surface underneath the electrical contacts had been slightly sanded prior to application of the electrical contacts. The four-probe method was used. The outer two contacts on each surface were 90 mm apart and were for passing current. The inner two contacts on each surface

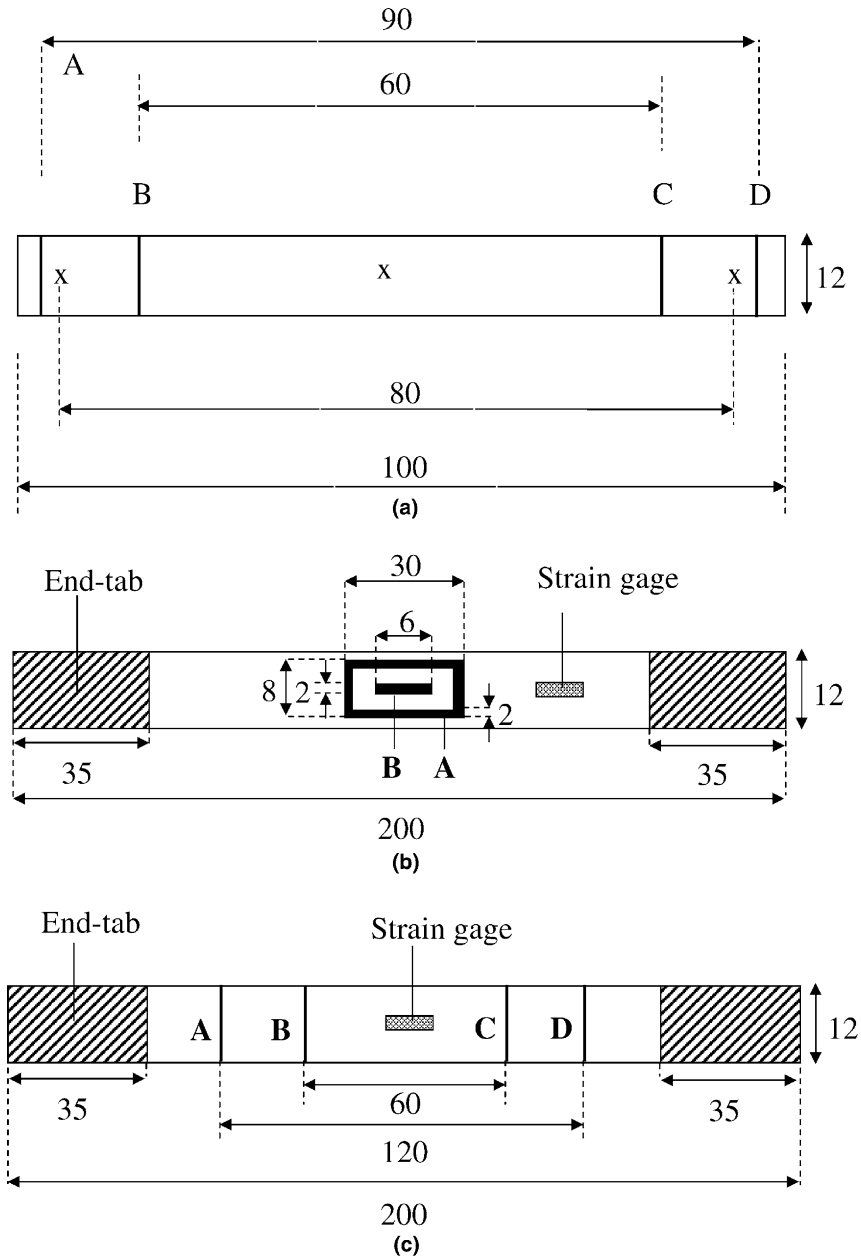


Fig. 2. Specimen configuration for self-sensing testing of laminate under, (a) three-point bending with measurement of surface resistances and oblique resistance, (b) uniaxial tension/compression with measurement of the through-thickness resistance and (c) uniaxial tension/compression with measurement of the longitudinal volume resistance. All dimensions are in mm. Electrical contacts on only one of the two opposite sides are shown. A, B, C and D are the electrical contacts for measurement of the resistance between B and C. The outer contacts (A and D) are for passing current. The inner contacts (B and C) are for voltage measurement. The X's indicate points for three-point bending, which was for the purpose of damage infliction.

were 60 mm apart and were for voltage measurement. A Keithley 2002 multimeter was used for resistance measurement.

To help explain the results of the flexural self-sensing demonstration described above, the through-thickness volume resistance was measured using the configuration of Fig. 2(b) and the longitudinal volume resistance was measured using the configuration of Fig. 2(c) during uniaxial tension (3 cycles) at a stress amplitude of +5.8 MPa, followed by uniaxial compression (3 cycles) at a stress amplitude of -5.8 MPa. In the configuration of Fig. 2(b), each of

the two current contacts is in the form of an open rectangle at the center of the specimen ($200 \times 12 \times 3.2$ mm), while each of the two voltage contacts is in the form of a solid small rectangle centered within the open rectangle mentioned above. Each of the two opposite surfaces has a current contact and a voltage contact, such that the corresponding contacts on the two surfaces are directly opposite each other. In the configuration of Fig. 2(c), each of the four electrical contacts is around the whole perimeter of the specimen in a plane that is perpendicular to the length of the specimen ($200 \times 12 \times 3.2$ mm). All contacts

in Fig. 2 are made of silver paint. At least two specimens were tested for each of the three configurations in Fig. 2 in order to show the general reproducibility of the results, though the data for a single specimen are presented for each configuration.

In order to assess the degree of damage resulting from flexural loading at various stress amplitudes, the flexural strength was measured after flexural loading at progressively increasing stress amplitudes (the series of values given above, with three cycles conducted at each stress amplitude) up to 476, 561 and 1000 MPa. Specimens subjected to static flexural loading up to failure for the purpose of measuring the flexural strength had experienced prior progressive flexural loading up to one of these three stress amplitude values. Three specimens were tested for each of the three highest stress amplitudes.

3. Results and discussion

3.1. Self-sensing under flexure

The surface resistance on the compression side decreased reversibly (Fig. 3(a)) while that on the tension side increased reversibly (Fig. 3(b)) in every stress cycle, even at the low maximum deflection of 0.249 mm (stress amplitude of 44.1 MPa). However, the oblique resistance did not show any systematic dependence on the deflection at this level of maximum deflection (Fig. 3(c)). At a maximum deflection of 0.521 mm (stress amplitude of

86.1 MPa), the oblique resistance as well as the surface resistance on the tension side increased reversibly with deflection, while the surface resistance on the compression side decreased reversibly (Fig. 4). Thus, it took higher deflection (stress) for the oblique resistance to start to change than for the surface resistances to start to change. At a maximum deflection of 0.724 mm, (stress amplitude of 129.7 MPa), the oblique resistance variation became clear, with relatively little noise (Fig. 5). In addition, both the peak and minimum values of the oblique resistance in a stress cycle decreased gradually cycle by cycle (Fig. 5(c)). At a maximum deflection of 1.199 mm (stress amplitude of 218.5 MPa), the oblique resistance started to decrease slightly upon loading prior to the abrupt increase upon subsequent greater loading (Fig. 6). This occurred at every stress cycle, thus resulting in the oblique resistance minimum to not coincide with the tension surface resistance minimum or the compression surface resistance maximum. This behavior is attributed to minor damage, which caused more touching between fibers of adjacent laminae and hence a lower oblique resistance. This minor damage was accompanied by the tension surface resistance curves becoming nonlinear (Fig. 6(b)). At a maximum deflection of 2.098 mm (stress amplitude of 392.3 MPa), the oblique resistance started to have a shoulder at the point of minimum deflection of a cycle (Fig. 7). The shoulder is attributed to the partially reversible nature of the minor damage mentioned above. This nature caused the oblique resistance to have a tendency to increase

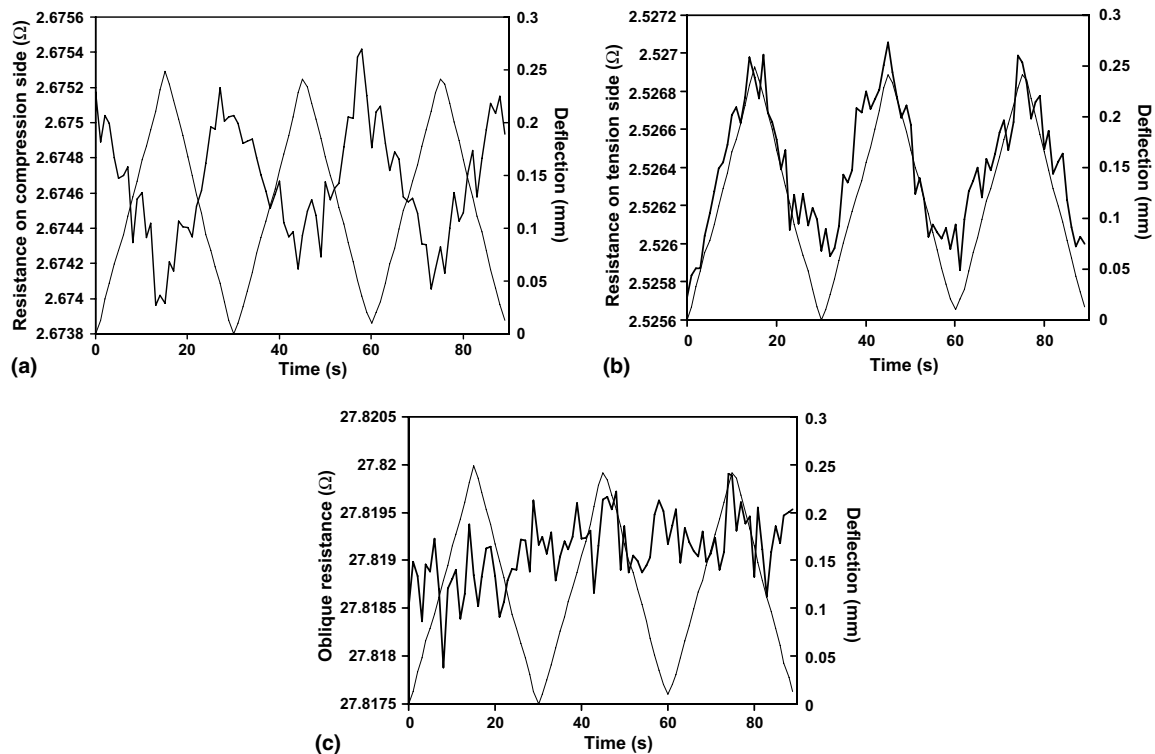


Fig. 3. Resistance (thick curve) during deflection (thin curve) cycling at a maximum deflection of 0.249 mm (stress amplitude of 44.1 MPa). (a) Compression surface resistance, (b) tension surface resistance and (c) oblique resistance.

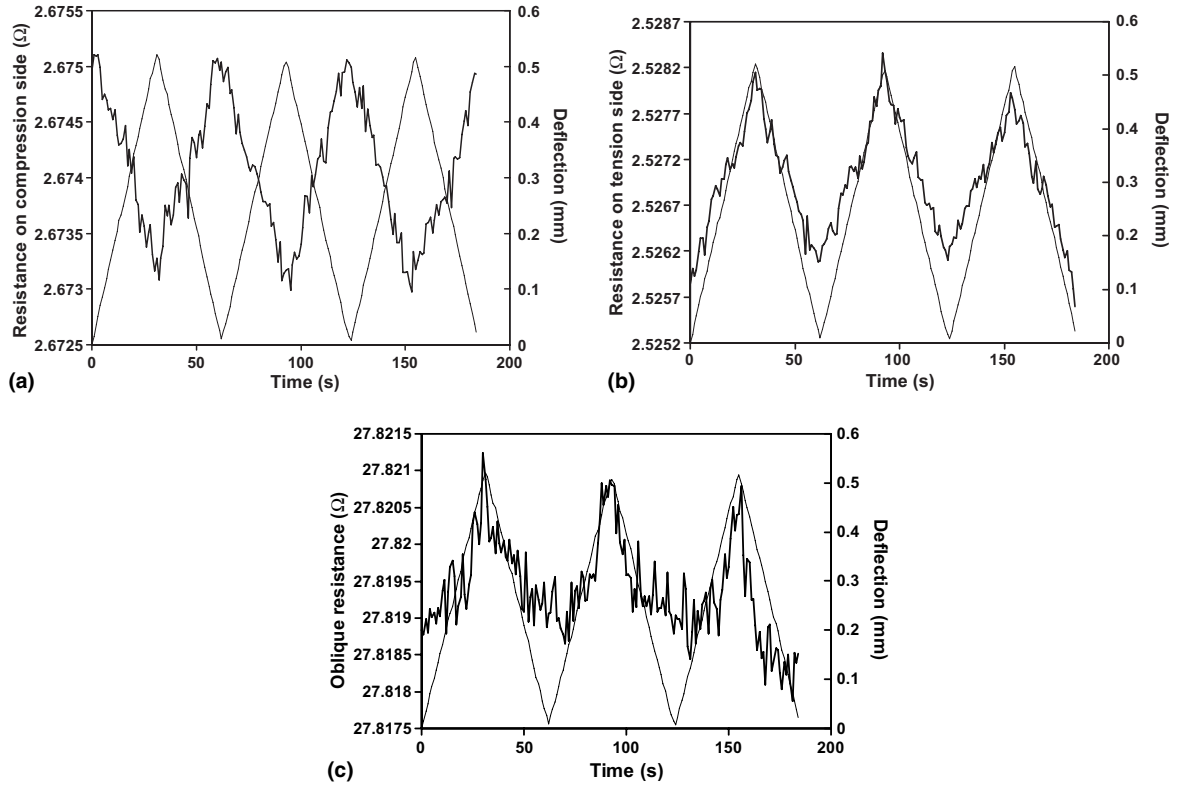


Fig. 4. Resistance (thick curve) during deflection (thin curve) cycling at a maximum deflection of 0.521 mm (stress amplitude of 86.1 MPa). (a) Compression surface resistance, (b) tension surface resistance and (c) oblique resistance.

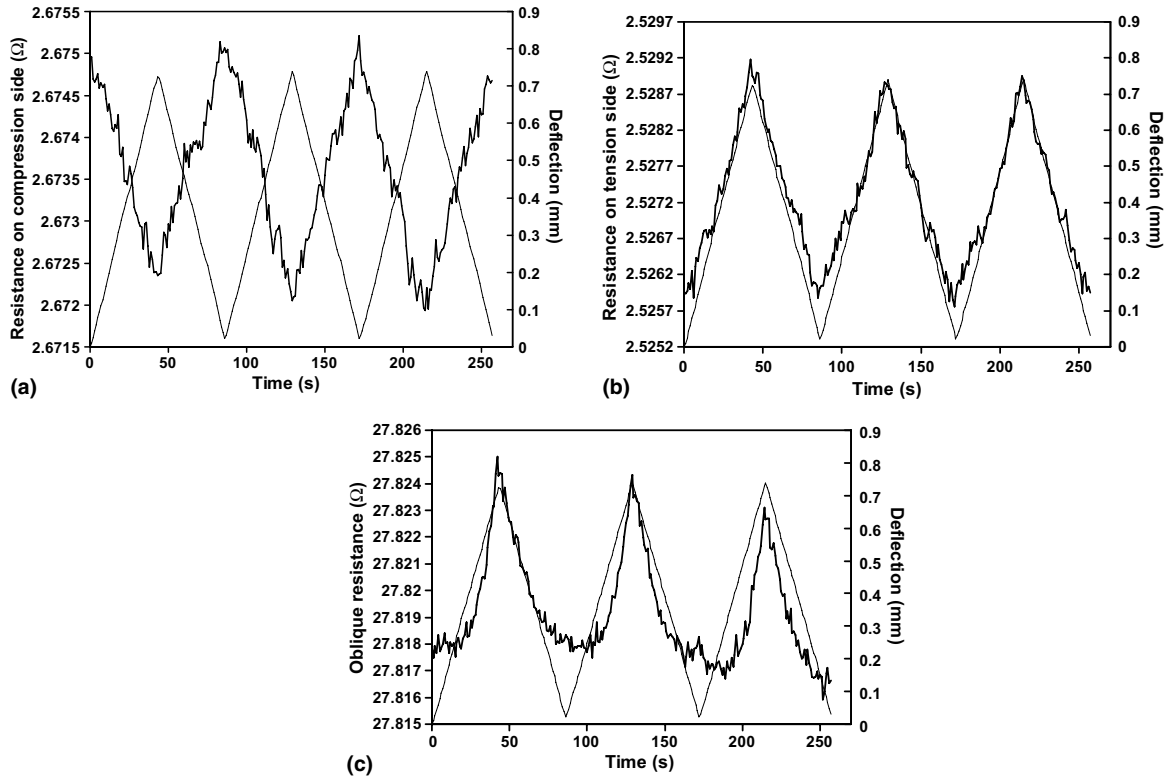


Fig. 5. Resistance (thick curve) during deflection (thin curve) cycling at a maximum deflection of 0.724 mm (stress amplitude of 129.7 MPa). (a) compression surface resistance, (b) tension surface resistance and (c) oblique resistance.

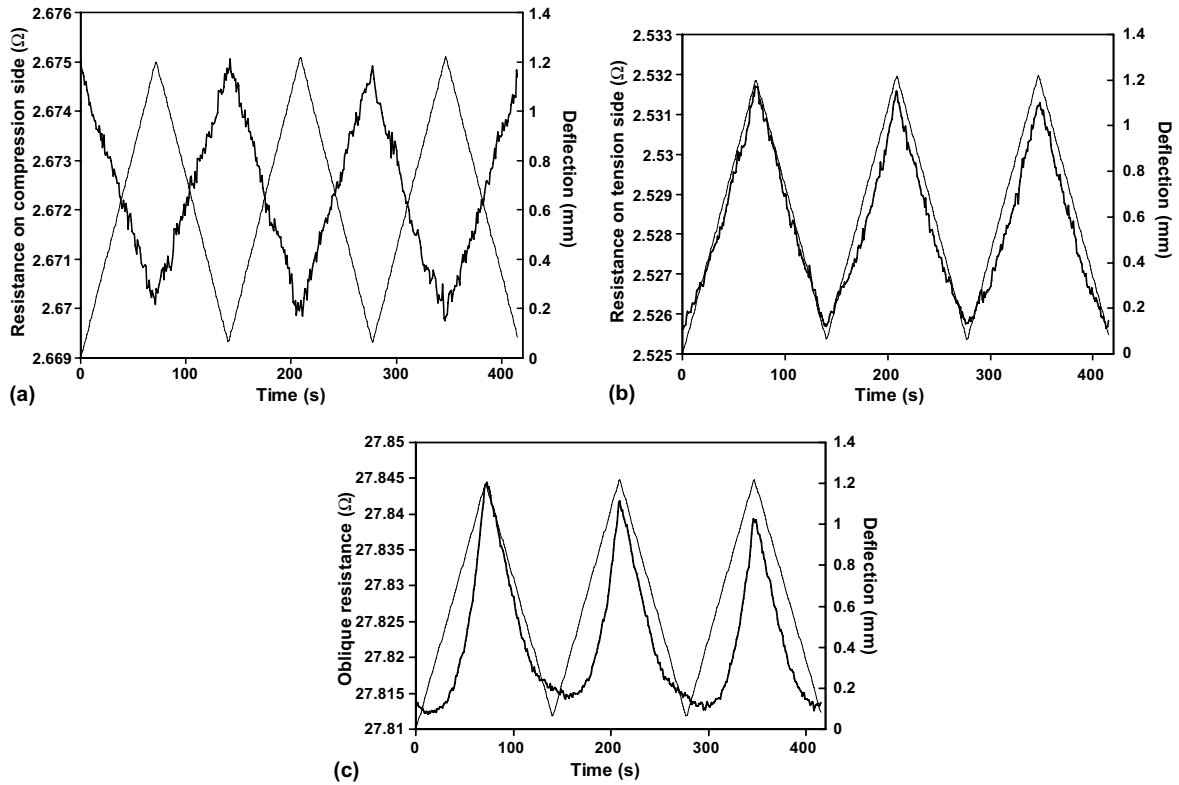


Fig. 6. Resistance (thick curve) during deflection (thin curve) cycling at a maximum deflection of 1.199 mm (stress amplitude of 218.5 MPa). (a) Compression surface resistance, (b) tension surface resistance and (c) oblique resistance.

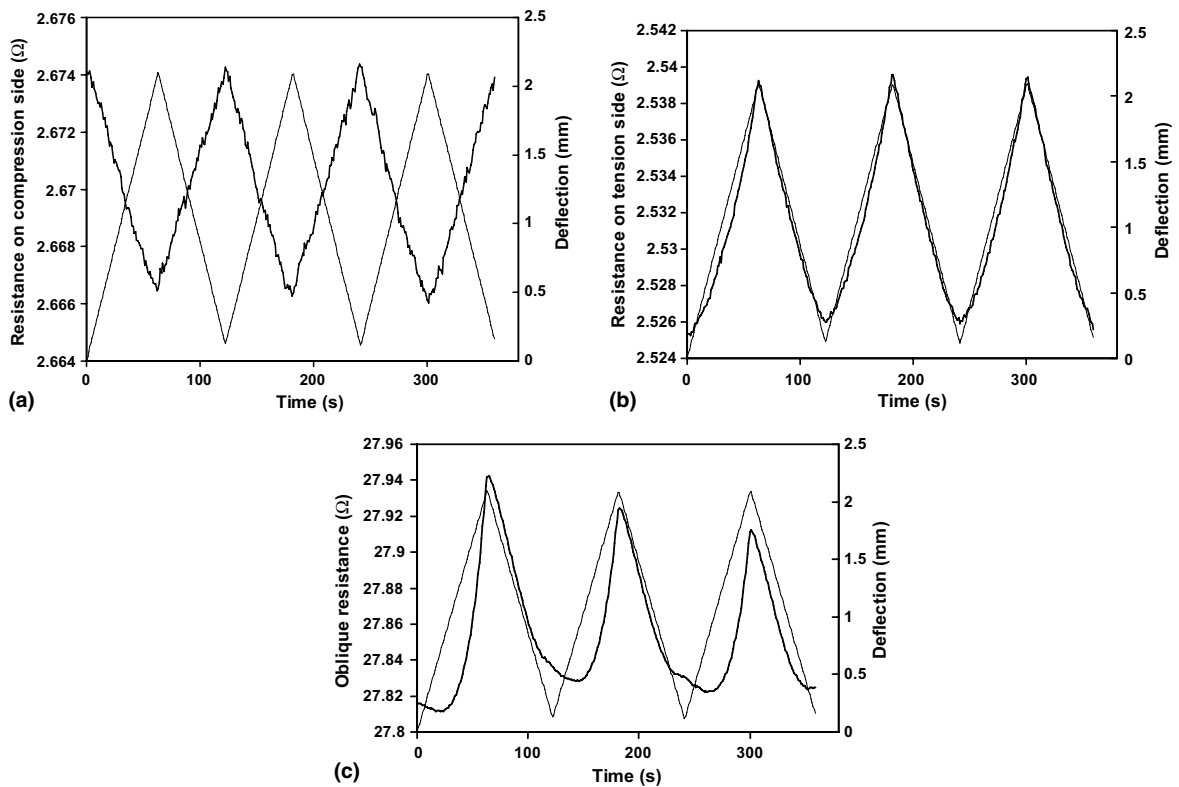


Fig. 7. Resistance (thick curve) during deflection (thin curve) cycling at an maximum deflection of 2.098 mm (stress amplitude of 392.3 MPa). (a) Compression surface resistance, (b) tension surface resistance and (c) oblique resistance.

slightly near the end of the unloading part of a stress cycle. As the maximum deflection further increased, the shoulder became clearer and evolved into a small peak (Fig. 8).

Due to the relative complexity of the variation in oblique resistance upon flexure, and due to the lower sensitivity to small deflections, the oblique resistance is not as attractive an indicator of strain than the tension/compression surface resistance. Since the strain is higher at the surface, it is reasonable that the surface resistance is a better indicator of strain than the oblique resistance.

As the maximum deflection increased, the nonlinearity occurred for the surface resistance of both compression and tension sides and became more and more severe, as shown in Figs. 8 and 9. At a maximum deflection of 4.945 mm, (stress amplitude of 996.2 MPa), the nonlinearity in the surface resistance of the tension side became so severe that the resistance increased with deflection abruptly at the start of loading, followed by a regime of gradual resistance increase (Fig. 9). This tendency for the tension surface resistance to increase more gradually is attributed to the increase in the degree of fiber alignment due to the tension causing the longitudinal resistivity to decrease, as previously reported for the case of uniaxial tension [11]. At a stress amplitude of 1045 MPa, major damage and failure occurred, as shown by abrupt increases in the three resistances accompanying abrupt decreases in stress, as shown in Fig. 10. The compression surface resistance and the oblique resistance showed abrupt increase before the

tension surface resistance. This is consistent with visual observation of cracking at the compression surface prior to cracking at the tension surface. It is also consistent with the fact that the oblique resistance probes the interior of the specimen, whereas the surface resistances probe the surface region only.

Upon flexure, the resistance increased for the tension surface and decreased for the compression surface. This is because of the decrease in the current penetration at the tension surface and the increase in the current penetration at the compression surface, as shown in the next section with through-thickness resistance data.

Upon flexure, the oblique resistance increased. This is due to the flexural strain, which caused a change in the geometry of the oblique current path. This path is not straight, due to the anisotropy of the composite. In other words, the current zigzags between the longitudinal direction and the through-thickness direction.

The oblique resistance after unloading decreased with increasing highest prior deflection for highest prior deflection of at least 2.5 mm (Fig. 11). This effect is accompanied by the slight decrease of the oblique resistance upon the start of loading and the appearance of a shoulder in the oblique resistance curve at the point where deflection is at its minimum in a cycle (Fig. 7(c)). These decreases in the oblique resistance are attributed to minor damage, which caused more fibers of one lamina to touch fibers of an adjacent lamina, thereby increasing the degree

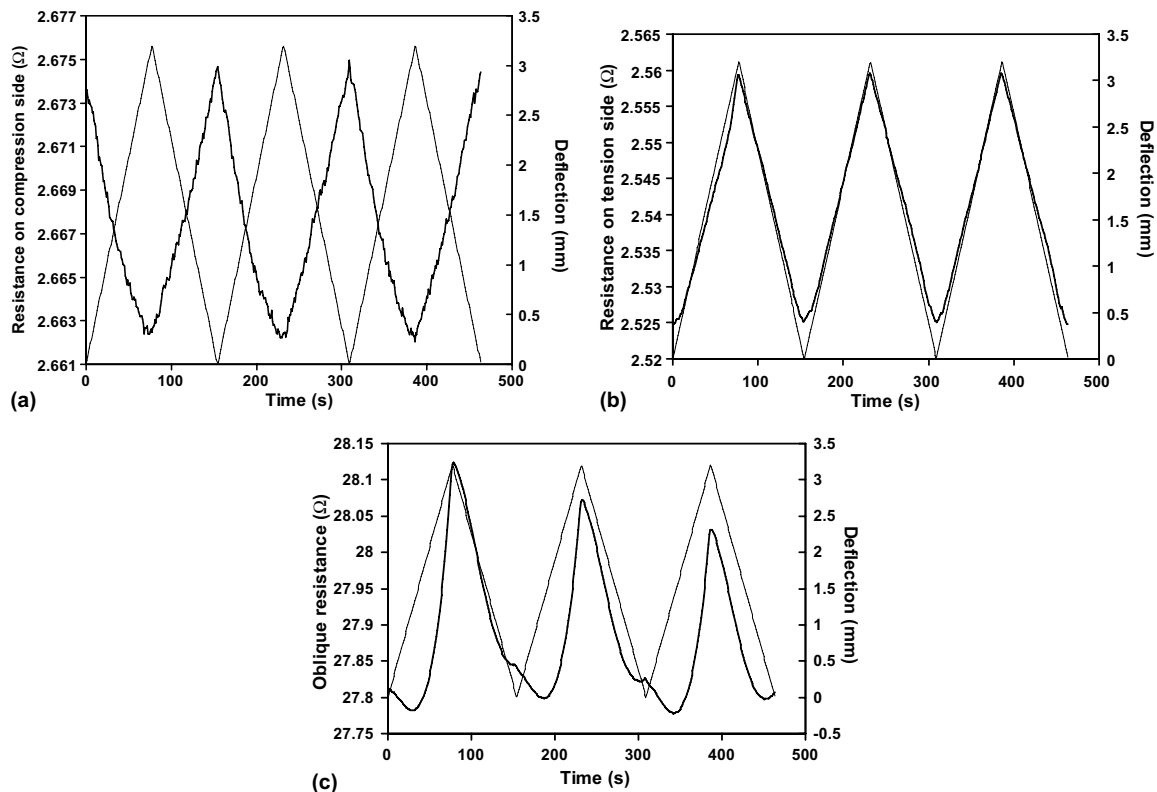


Fig. 8. Resistance (thick curve) during deflection (thin curve) cycling at an maximum deflection of 3.198 mm (stress amplitude of 650.7 MPa). (a) Compression surface resistance, (b) tension surface resistance and (c) oblique resistance.

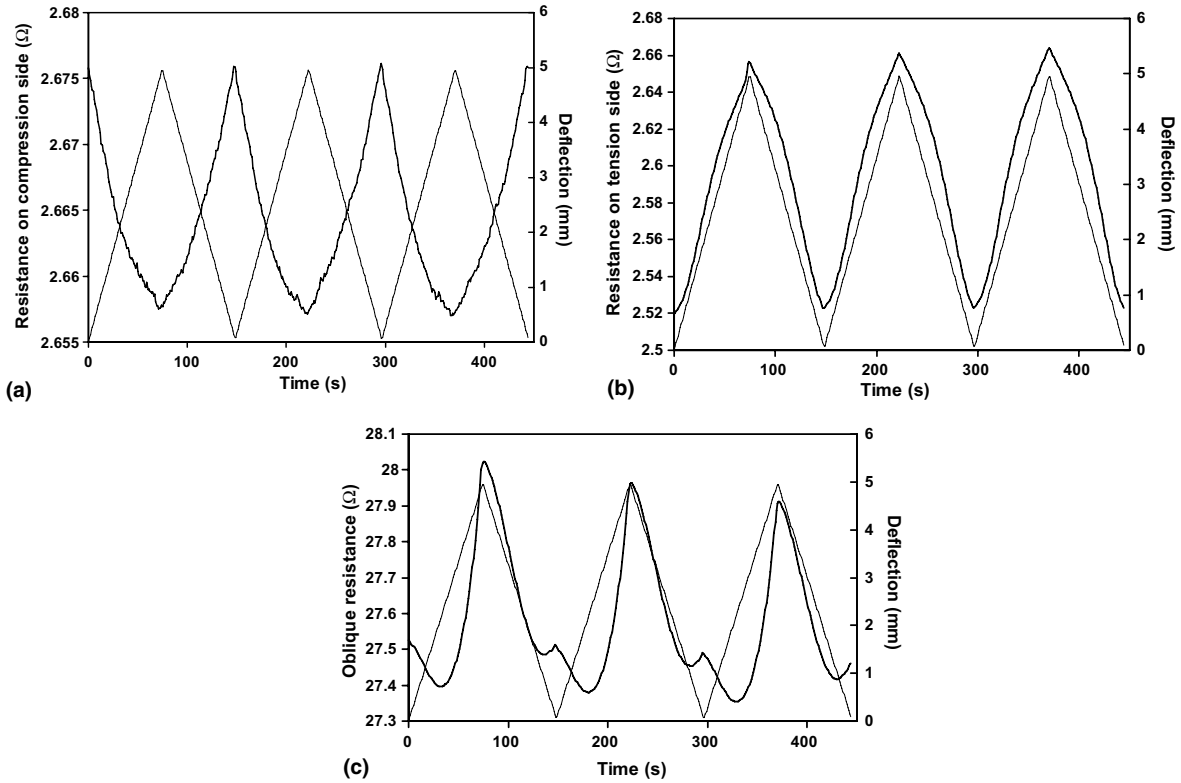


Fig. 9. Resistance (thick curve) during deflection (thin curve) cycling at an maximum deflection of 4.945 mm (stress amplitude of 996.2 MPa). (a) Compression surface resistance, (b) tension surface resistance and (c) oblique resistance.

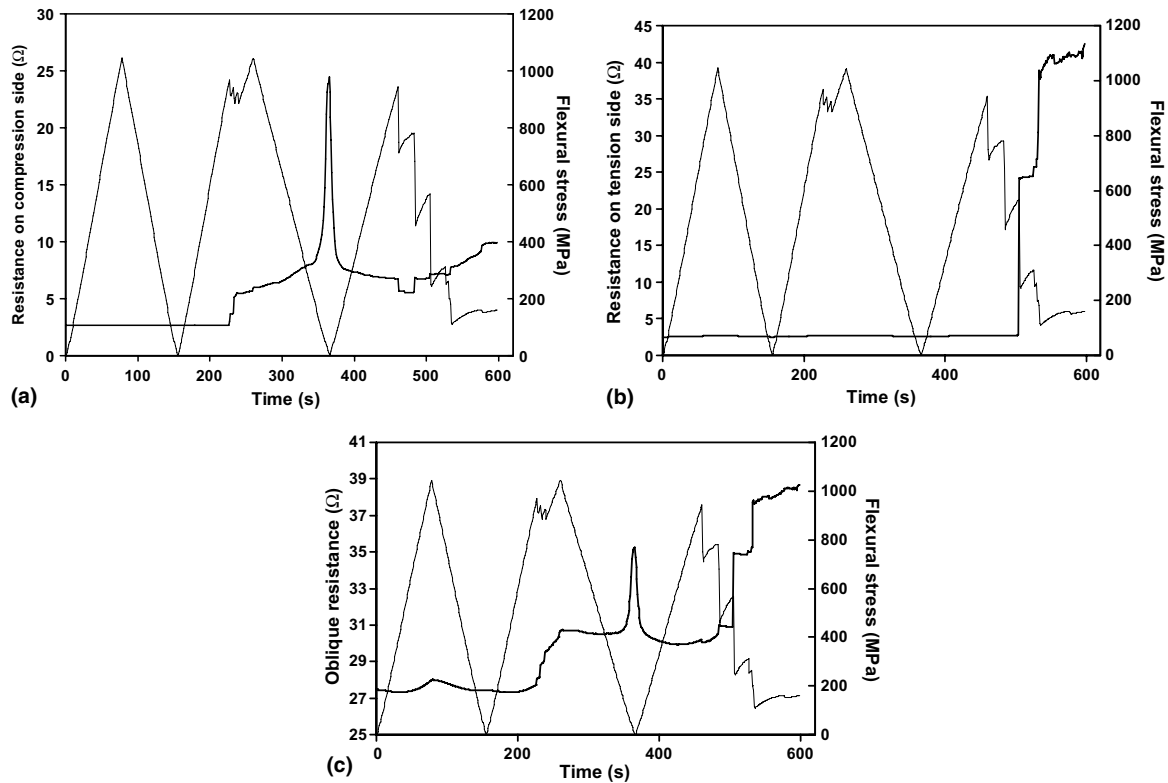


Fig. 10. Resistance (thick curve) during flexural stress (thin curve) cycling at an intended stress amplitude of 1045.1 MPa and an intended maximum deflection of 5.194 mm. (a) Compression surface resistance, (b) tension surface resistance and (c) oblique resistance.

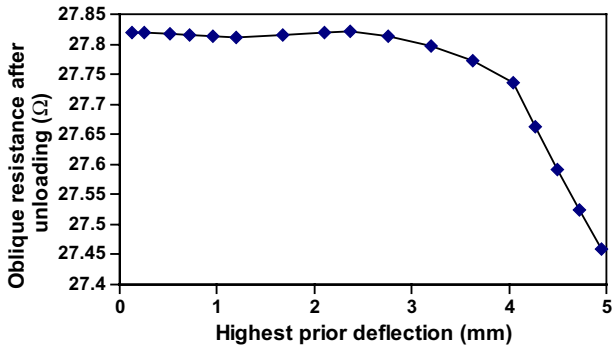


Fig. 11. Oblique resistance after unloading vs. highest prior deflection.

of current penetration. This means that the oblique resistance at zero load may serve as an indicator of damage.

This indicator is more amenable for practical implementation than the decrease of the oblique resistance upon the start of loading of the size of the shoulder in the oblique resistance curve. The oblique resistance is a better indicator of damage than the tension/compression surface resistance, because it probes the interior of the specimen, whereas the surface resistance probes the surface region only.

Fig. 12 shows a superposition of the curves of resistance vs. deflection during the first loading at each of the progressively increasing values of the maximum stress/deflection. For the surface resistance of the compression/tension side and for the oblique resistance, the curves were linear up to a maximum deflection of about 1.5 mm, beyond which the curves became increasingly nonlinear. For the oblique resistance (Fig. 12(c)), the resistance of the unloaded state

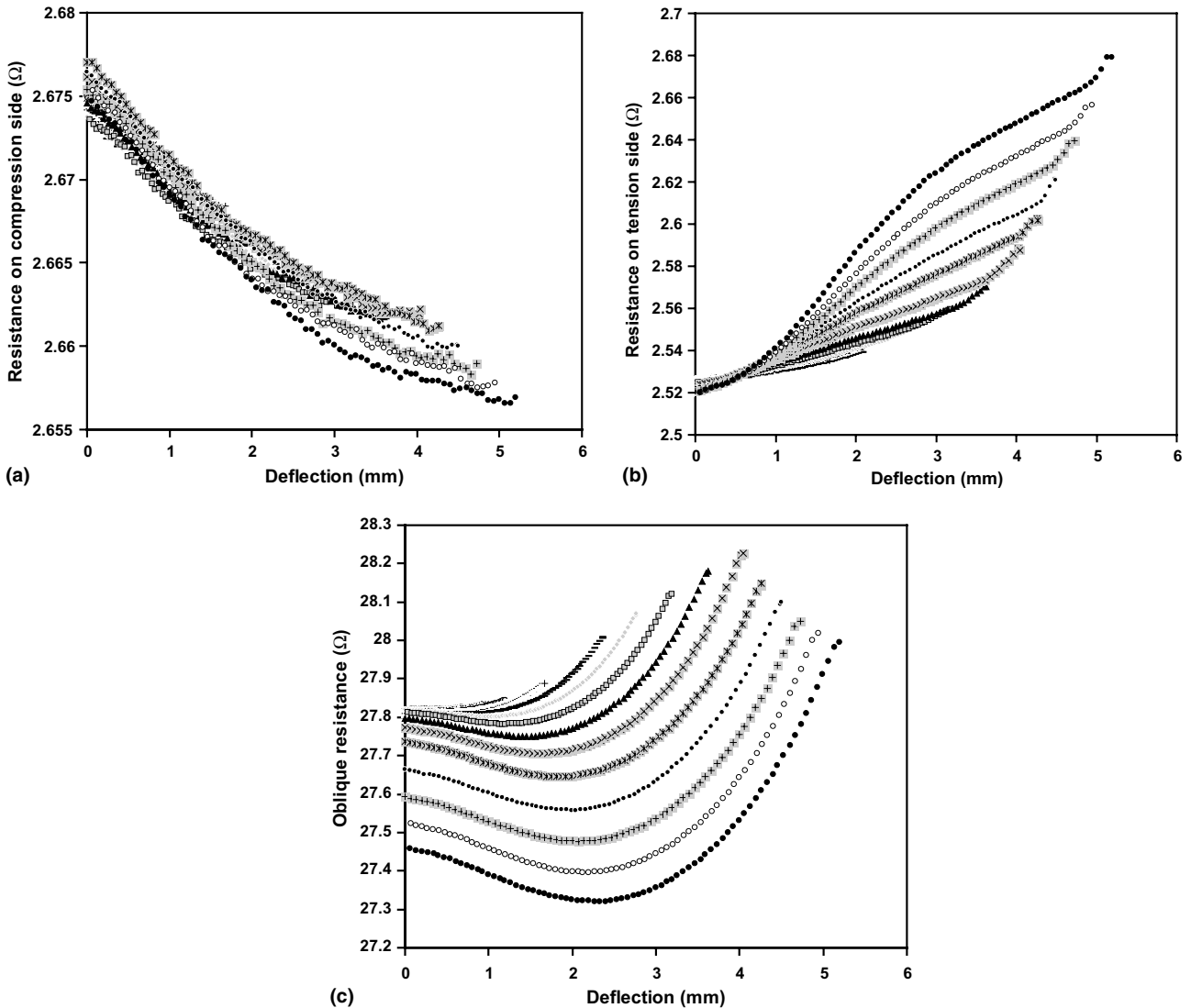


Fig. 12. Resistance vs. deflection during the first loading at progressively increasing values of the maximum stress/deflection. The maximum stress is indicated below. The maximum deflection is the deflection at the end of corresponding curve. (a) Compression surface resistance, (b) tension surface resistance and (c) oblique resistance. \diamond 21 MPa \square 44 MPa \triangle 86 MPa \times 130 MPa $*$ 175 MPa \oplus 218 MPa $+$ 305 MPa $-$ 392 MPa $-$ 477 MPa \diamond 562 MPa \blacksquare 651 MPa \blacktriangle 738 MPa \boxtimes 825 MPa \boxplus 866 MPa \bullet 911 MPa \boxminus 956 MPa \diamond 996 MPa \blacklozenge 1045 MPa.

progressively decreased as the highest prior deflection increased. A similar but much smaller decrease was observed for the surface resistance of the tension side (Fig. 12(b)). This effect was not consistently observed for the surface resistance of the compression side (Fig. 12(a)). In the nonlinear regime, the curve of the resistance vs. deflection exhibited inflection for the tension surface resistance and the oblique resistance. The inflection in the curve for the tension surface resistance is due to the tendency for this resistance to increase only gradually at a high deflection (Fig. 9(b)). The inflection in the curve for the oblique resistance is due to the slight decrease in oblique resistance in the regime of low deflection in the presence of minor damage (Figs. 6(c), 7(c), 8(c) and 9(c)).

The decrease of the oblique resistance after unloading with increasing highest prior deflection (Fig. 12(c)) is consistent with the behavior shown in Fig. 11. It is attributed to minor damage, which causes more contact between fibers of adjacent laminae, as explained in relation to Fig. 11.

The small decrease of the resistance on the tension side after unloading with increasing highest prior deflection (Fig. 12(b)) is probably due to irreversible and slight decrease of the degree of 0° fiber alignment after the distur-

bance associated with a deflection cycle and the consequent increase in the current penetration. The higher is the maximum deflection, the more is the disturbance and the greater is this minor effect.

Consistent with Figs. 12 and 13(a) shows that the magnitude of the maximum reversible fractional change in resistance increased with increasing maximum deflection (or stress amplitude) for the compression/tension surface resistance and the oblique resistance. In case of the oblique resistance, a slight drop in the maximum fractional reversible resistance change was consistently observed in the regime of high maximum deflection (4 mm in Fig. 13(c)). This drop is probably due to damage infliction, which causes more contact between fibers of adjacent laminae, thereby decreasing the oblique resistance.

From a practical viewpoint, the results mean that the composite is effective for strain/stress sensing and damage sensing under flexure. Strain/stress sensing involves measurement of the resistance of either the tension surface or the compression surface and using Fig. 13(a) and (b) as calibration curves. The sensing of minor damage involves measurement of the oblique resistance and using Fig. 11 as a calibration curve.

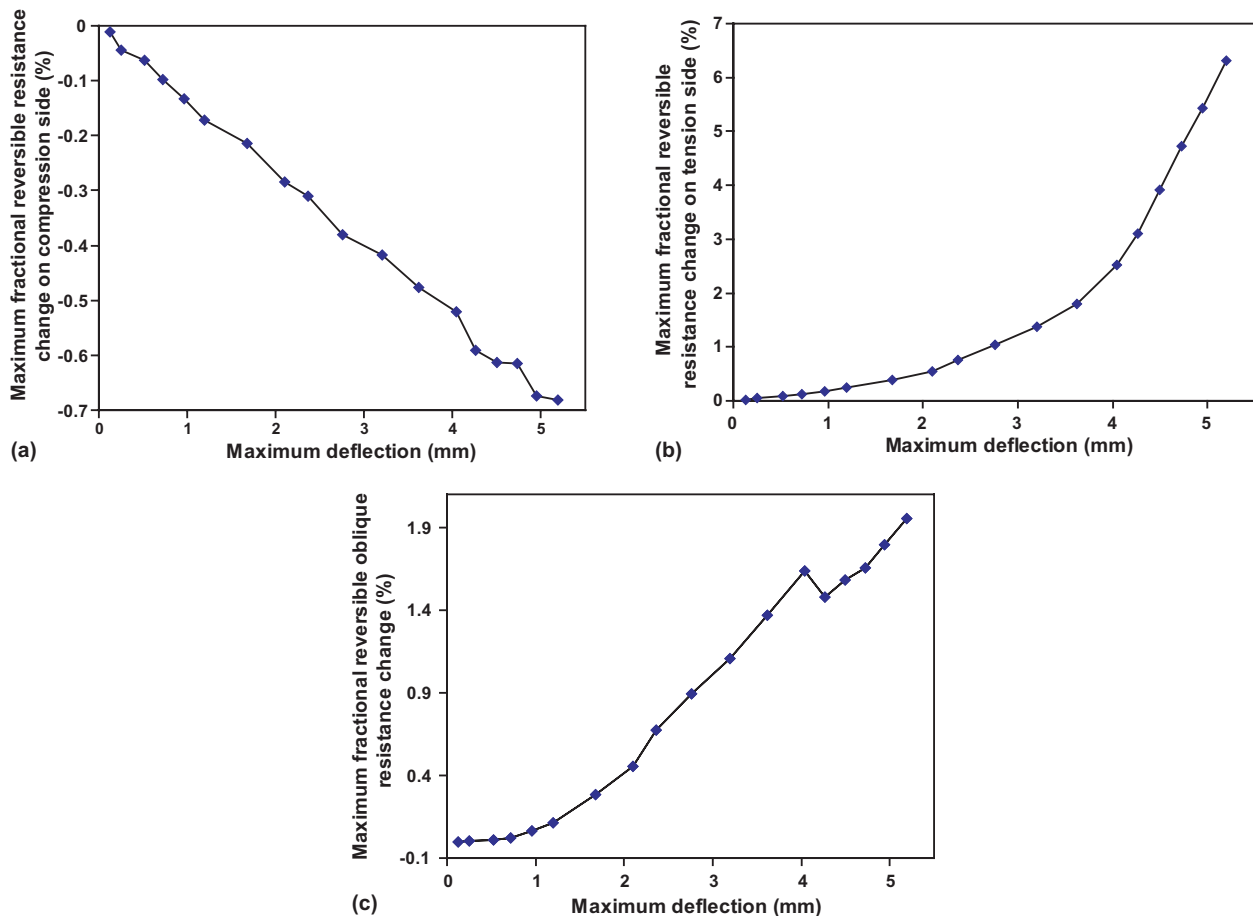


Fig. 13. Maximum fractional reversible resistance change vs. the maximum deflection. (a) Compression surface resistance, (b) tension surface resistance and (c) oblique resistance.

3.2. Self-sensing under uniaxial tension and compression

Fig. 14(a) and (b) show that the through-thickness resistance increases upon uniaxial tension (+5.8 MPa) and decreases upon uniaxial compression (−5.8 MPa) respectively. Fig. 15(a) and (b) show that the longitudinal volume resistance does not change upon uniaxial tension (+5.8 MPa) or uniaxial compression (−5.8 MPa). The difference in resistance scale between Figs. 14 and 15 should be noted. Comparison of Figs. 14 and 15 shows that the through-thickness resistance variation upon uniaxial loading is much more significant than the longitudinal resistance variation upon the same loading. Thus, the tension surface resistance increase observed upon flexure (last section) is due to the increase in the through-thickness resistance and the consequent decrease in the current penetration, while the compression surface resistance decrease observed upon flexure (last section) is due to the decrease in the through-thickness resistance and the consequent increase in the current penetration.

Fig. 14(a) also shows that the through-thickness resistance decreases irreversibly at the first stress cycle. This decrease results in an increase in the current penetration

and hence a small decrease in the tension surface resistance under flexure (as shown in Fig. 12(b)).

3.3. Damage degree assessment

The flexural strength loss increased with increasing highest stress amplitude such that the fractional loss in flexural strength was up to 6.5%, which was the value for the highest stress amplitude of 1000 MPa. This stress amplitude is close to that in Fig. 9, where the surface resistance variation with deflection shows nonlinearity and the shoulder in the oblique resistance variation becomes a clear peak. This means that the damage corresponding to such resistance behavior is minor, in contrast to the major damage at the stress amplitude of 1045 MPa (Fig. 10).

Visible cracking and sound emission occurred only for the highest stress amplitude of 1000 MPa. They did not occur for the highest stress amplitude of 561 or 476 MPa. For the stress amplitude of 1000 MPa, sound was not heard during the first cycle, but was heard during the second cycle. The sound emission was accompanied by a slight drop in the flexural stress, which indicates a slight decrease in the load carrying capacity. The crack observed by the

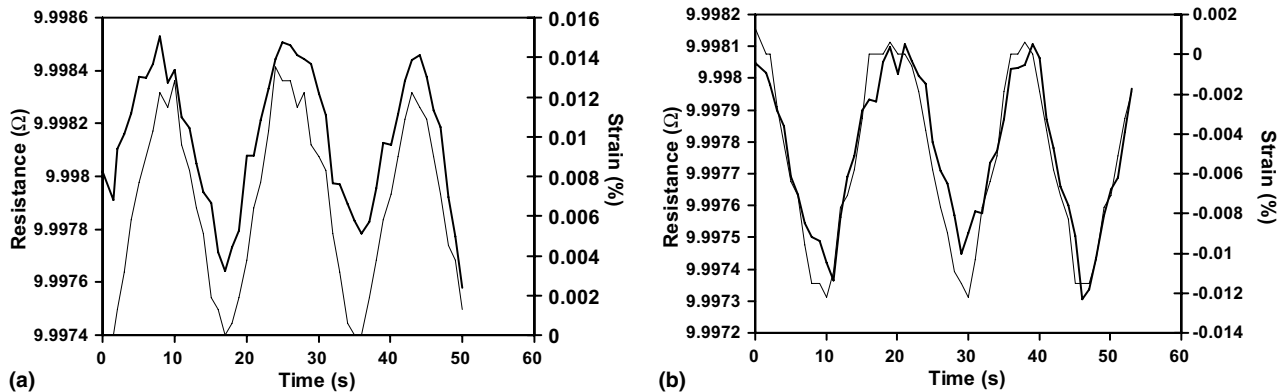


Fig. 14. Through-thickness resistance during uniaxial loading. (a) Uniaxial tension at a stress amplitude of +5.8 MPa and (b) uniaxial compression at a stress amplitude of −5.8 MPa.

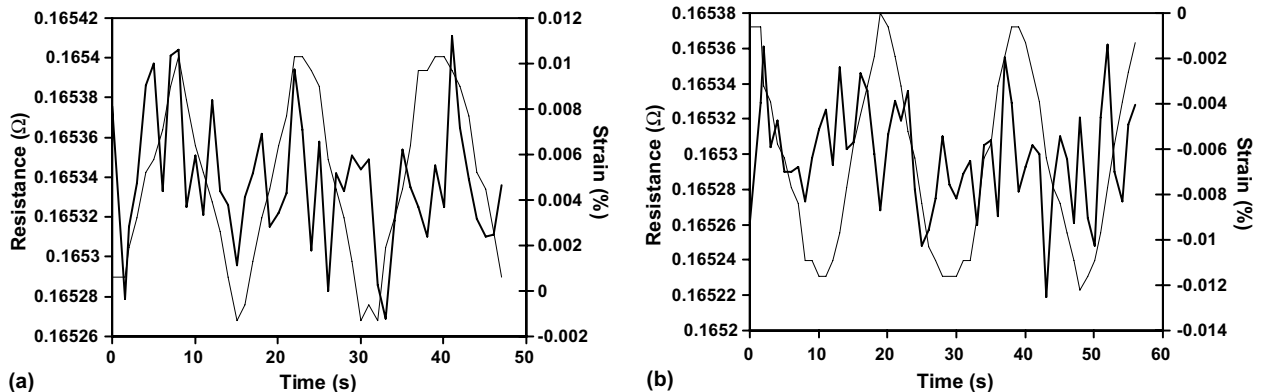


Fig. 15. Longitudinal volume resistance during uniaxial loading. (a) Uniaxial tension at a stress amplitude of +5.8 MPa and (b) uniaxial compression at a stress amplitude of −5.8 MPa.

naked eyes after the stress cycling at 1000 MPa was in the form of a line (not perfectly straight) along the whole width of the specimen at the middle of the specimen on the compression surface only. No crack was observed on the tension surface. That damage was not observed on the tension surface is consistent with Fig. 10, which shows that the resistance on the compression side started to increase abruptly before the resistance on the tension side started to increase abruptly.

Since there are 24 laminae in the composite, the incapacitation of one lamina due to cracking in the lamina may be roughly estimated to cause a strength loss of 1/24 or 4.2%. However, this estimation does not take into account the fact that damage of the surface region of the outermost lamina affects the flexural strength more than damage of the interior region of this lamina. Thus, the strength loss of 6.5% suggests that the damage mainly occurs in the outermost lamina.

4. Conclusion

Self-sensing under flexure has been demonstrated in carbon fiber polymer-matrix composite by measurement of the DC electrical resistances during flexure. The resistance of the compression surface decreases reversibly upon flexure, due to strain-induced increase in the degree of current penetration; the resistance of the tension surface increases reversibly, due to strain-induced decrease in the degree of current penetration; the oblique resistance increases reversibly, due to flexural strain. The tension/compression surface resistance is a better indicator of strain than the oblique resistance, as it is more sensitive to low deflections and depends on the deflection in a simpler fashion.

Minor damage that is at most in the form of cracking at the compression surface to a depth of about a single lamina is indicated by the variation of the resistance (both tension and compression surfaces) with deflection becoming nonlinear. The degree of nonlinearity increases with the maximum deflection. However, minor damage is more conveniently indicated by the oblique resistance. Specifically, it is indicated by (i) the oblique resistance after unloading decreasing, (ii) the oblique resistance during loading decreasing near the start of flexural loading, and (iii) the appearance of a shoulder in the oblique resistance curve at the point where the deflection is minimum in a cycle.

Major damage close to failure is indicated by the tension and compression surface resistances and the oblique resistance increasing abruptly and irreversibly. The onset of this abrupt increase occurs earlier for the compression surface resistance and the oblique resistance than the tension surface resistance.

References

[1] Clerico M, Ruvinetti G, Cipri F, Pelosi M. Analysis of impact damage and residual static strength in improved CFRP [carbon fiber-reinforced plastics]. *Int J Mater Prod Technol* 1989;4(1):61–70.

[2] Haque A, Raju PK. Monitoring fatigue damage in carbon fiber composites using an acoustic impact technique. *Mater Eval* 1998;56(6):765–70.

[3] Verma RK, Kander RG, Hsiao BS. Acoustic emission monitoring of damage using high amplitude gains in carbon fiber reinforced poly(ether ketone ketone). *J Mater Sci Lett* 1994;13(6):438–42.

[4] De Freitas M, Silva A, Reis L. Numerical evaluation of failure mechanisms on composite specimens subjected to impact loading. *Compos Part B-Eng* 2000;31(3):199–207.

[5] Rose JL, Rajana KM, Barshinger JN. Guided waves for composite patch repair of aging aircraft. *Rev Progress Quant Non-destructive Eval* 1996;15B:1291–8.

[6] Sjogren A, Krasnikovs A, Varna J. Experimental determination of elastic properties of impact damage in carbon fibre/epoxy laminates. *Compos Part A-Appl S* 2001;32(9):1237–42.

[7] Abry JC, Bocharard S, Chateauminois A, Salvia M, Giraud G. In situ detection of damage in CFRP laminates by electrical resistance measurements. *Compos Sci Technol* 1999;59(6):925–35.

[8] Abry JC, Choi YK, Chateauminois A, Dalloz B, Giraud G, Salvia M. In situ monitoring of damage in CFRP laminates by means of AC and DC measurements. *Compos Sci Technol* 2001;61(6):855–64.

[9] Ceysson O, Salvia M, Vincent L. Damage mechanisms characterization of carbon fibre/epoxy composite laminates by both electrical resistance measurements and acoustic emission analysis. *Scripta Mater* 1996;34(8):1273–80.

[10] Chu Y-W, Yum Y-J. Detection of delamination in graphite/epoxy composite by electric potential method. *Proceedings – KORUS 2001*, In: The 5th Korea–Russia international symposium on science and technology, Section 5 – Mechanics and Automotive Engineering, p. 240–2.

[11] Chung DDL, Wang S. Self-sensing of damage and strain in carbon fiber polymer-matrix structural composites by electrical resistance measurement. *Polym Polym Compos* 2003;11(7):515–25.

[12] Irving PE, Thiagarajan C. Fatigue damage characterization in carbon fibre composite materials using an electrical potential technique. *Smart Mater Struct* 1998;7:456–66.

[13] Kaddour AS, Al-Salehi AR, Al-Hassani STS, Hinton MJ. Electrical resistance measurement technique for detecting failure in CFRP materials at high strain rates. *Compos Sci Technol* 1994;51(3):377–85.

[14] Kupke M, Schulte K, Schüler R. Non-destructive testing of FRP by DC and AC electrical methods. *Compos Sci Technol* 2001;61:837–47.

[15] Mei Z, Guerrero VH, Kowalik DP, Chung DDL. Mechanical damage and strain in carbon fiber thermoplastic-matrix composite, sensed by electrical resistivity measurement. *Polym Compos* 2002;23(3):425–32.

[16] Muto N, Yanagida H, Nakatsuji T, Sugita M, Ohtsuka Y, Arai Y. Design of intelligent materials with self-diagnosing function for preventing fatal fracture. *Smart Mater Struct* 1992;1:324–9.

[17] Muto N, Yanagida H, Nakatsuji T, Sugita M, Ohtsuka Y, Arai Y, et al. Materials design of CFGFRP-reinforced concretes with diagnosing function for preventing fatal fracture. *Adv Compos Mater* 1995;4(4):297–308.

[18] Prabhakaran R. Damage assessment through electrical resistance measurement in graphite fiber-reinforced composites. *Exp Techniques* 1990;14(1):16–20.

[19] Schulte K. Damage monitoring in polymer-matrix structures. *J Phys III Colloque C7* 1993;3:1629–36.

[20] Todoroki A, Kobayashi H, Matuura K. Application of electric potential method to smart composite structures for detecting delamination. *JSME Int J A—Solid M* 1995;38(4):524–30.

[21] Sugita M, Yanagida H, Muto N. Materials design for self-diagnosis of fracture in CFGFRP composite reinforcement. *Smart Mater Struct* 1995;4(1A):A52–7.

[22] Wang S, Shui X, Fu X, Chung DDL. Early fatigue damage in carbon fiber composites, observed by electrical resistance measurement. *J Mater Sci* 1998;33(15):3875–84.

[23] Wang S, Chung DDL. Mechanical damage in carbon fiber polymer-matrix composite, studied by electrical resistance measurement. *Compos Interf* 2002;9(1):51–60.

- [24] Wang S, Kowalik DP, Chung DDL. Self-sensing attained in carbon fiber polymer-matrix structural composites by using the interlaminar interface as a sensor. *Smart Mater Struct* 2004;13(3):570–92.
- [25] Wang S, Mei Z, Chung DDL. Interlaminar damage in carbon fiber polymer-matrix composites, studied by electrical resistance measurement. *Int J Adh Adh* 2001;21(ER6):465–71.
- [26] Wang X, Fu X, Chung DDL. Electromechanical study of carbon fiber composites. *J Mater Res* 1998;13(11):3081–92.
- [27] Wang X, Wang S, Chung DDL. Sensing damage in carbon fiber and its polymer-matrix and carbon-matrix composites by electrical resistance measurement. *J Mater Sci* 1999;34(11):2703–14.
- [28] Wang X, Chung DDL. Fiber breakage in polymer-matrix composite during static and dynamic loading, studied by electrical resistance measurement. *J Mater Res* 1999;14(11):4224–9.
- [29] Yoshitake K, Shiba K, Suzuki M, Sugita M, Okuhara Y. Damage evaluation for concrete structures using fiber reinforced composites as self-diagnosis materials. In: Udd E, Inaudi D, editors. *Smart structures and materials 2004: smart sensor technology and measurement systems*. Proceedings of SPIE, vol. 5384. Bellingham (WA): SPIE; 2004. p. 89–97.
- [30] Wen S, Chung DDL. Strain sensing characteristics of carbon fiber reinforced cement. *ACI Mater J* 2005;102(4):244–8.
- [31] Chung DDL. Damage in cement-based materials, studied by electrical resistance measurement. *Mater Sci Eng R* 2003;42(1):1–40.
- [32] Wen S, Chung DDL. A comparative study of steel- and carbon-fibre cement as piezoresistive strain sensors. *Adv Cem Res* 2003;15(3):119–28.
- [33] Chung DDL. Piezoresistive cement-based materials for strain sensing. *J Intel Mater Syst Str* 2002;13(9):599–609.
- [34] Wen S, Chung DDL. Uniaxial tension in carbon fiber reinforced cement, sensed by electrical resistivity measurement in longitudinal and transverse directions. *Cem Concr Res* 2000;30(8):1289–94.
- [35] Wang S, Chung DDL, Chung JH. Impact damage of carbon fiber polymer-matrix composites, monitored by electrical resistance measurement. *Compos Part A—Appl S* 2005;36:1707–15.